Turing-type Transients as a Model of Slow Voltage Shifts in Human Brain Activity

Gerold Baier[1,(*)], Lixue Qi[2], Liyuan Zhang[3], Jiajie Mo[4], Kai Zhang[4], Qingyun Wang[5], and Denggui Fan[2]

[1]*Cell and Developmental Biology, University College London, London, WC1E 6BT, UK*

[2]*Department of Mathematics and Physics, University of Science and Technology Beijing, 100083, Beijing, China*

[3]*Department of Biomedical Engineering, Faculty of Environment and Life, Beijing University of Technology, 100124, Beijing, China*

[4]*Department of Neurosurgery, Beijing Tiantan Hospital, Capital Medical University of Technology, 100070, Beijing, China*

[5]*Department of Dynamics and Control, Beihang University, 100191, Beijing, China*

Abstract

Slow potential shifts are spatially localised irregular temporal patterns observed in invasive electroencephalogram (EEG) in humans. Presently, their dynamic origin is not understood. We study a coupled canonical neural population model which lacks slow shift components. We find that the inclusion of inhibitory cross-coupling leads to a subcritical Turing instability resulting in a tri-stable situation with spatial symmetry breaking. Near this bifurcation the background state is excitable, and pulse-perturbations lead to prolonged spatially asymmetric transients. In the presence of noise, localised slow shifts appear transiently in the time series. In the EEG, electrical stimulation can probe for the presence of this Turing excitability. Given their partly deterministic nature, Turing transients could play a role in cognitive processes like decision making.

Lead Paragraph

Localised slow voltage shifts have long been observed in the human brain activity in the context of cognitive processes. Here we propose a new dynamic mechanism for this phenomenon. Dynamical systems modelling shows that cross-inhibitory coupling between nearby locations in the brain leads to spatial pattern formation and a new type of tissue excitability with spatially localised transient potential shifts. We propose a clinically feasible way to test for their presence (or absence) in humans and suggest a functional role of these shifts in information processing in the human brain.

[*)] Email: g.baier@ucl.ac.uk

I. INTRODUCTION

Slow electric potential shifts recorded in invasive or stereo electroencephalography (sEEG) in humans have received attention in the context of neurosurgery [1]. They are spatially asymmetric, transients that appear either spontaneously or near the start of epileptic seizures [2]. They are found as slow large-amplitude fluctuations in various cerebral locations on top of a common irregular background, particularly if the sEEG is viewed in the bipolar montage (potential recorded as the difference between two adjacent contacts of sEEG electrodes) [3]. While slow shifts, also referred to as direct current (DC) shifts, may be recording artifacts in surface EEG (electrodes attached to the skin), they are considered genuine in invasive recordings where electrode contacts are within the brains electrolyte environment [2]. They are also found in magnetoencephalography, with better brain localisation capability as compared to surface EEG [4]. In spite of evidence that slow shifts may result from cognitive brain processes [5, 6], the dynamic origin of slow potential shifts is not known presently [7]. This is unsatisfactory in the light of their potential use for mapping the epileptogenic zone in epilepsy surgery [8]; their potential use in brain-computer interfaces [9]; and their appearance in response to sensory stimulation [10] which indicates a role in information processing in the healthy brain. Fig. 1 shows a low-pass filtered sEEG time series with and without slow potential shifts.

The most reliable source of slow potential shifts is the invasive EEG in patients undergoing presurgical monitoring. Studies of invasive recordings have confirmed that they are not artifacts and that they may correlate with the occurrence of focal-onset epileptic seizures [7]. In the context of seizure onset, they were assigned the role as an abstract slow process which drives a nonlinear system across bifurcations to seizure rhythms [11],[12]. None of the proposed bifurcations, however, included any spatial symmetry breaking. In spatio-temporal models, instabilities resulted in deterministic oscillatory activity that spread to neighboring locations, both in continuous neural field models [13] and in discontinuous network models [14]. Spatial symmetry-breaking of Turing-type was observed in stationary patterns in a model of slow-wave sleep oscillations where it led to complex cortical patterns when combined with a Hopf bifurcation in partial differential equations [15]. An important feature of such solutions is that they can account for localisation. However, they do not explain the irregular temporal features of slow potential shifts in humans.

We study a minimal model of the electric activity in two spatially close cortical (or subcortical) units and the impact of inhibitory cross-coupling between these units in accordance with known neurophysiological coupling schemes. We find that inhibitory cross-coupling leads to spatial symmetry breaking solutions and a novel type of excitability. We propose this excitability as a testable hypothesis for slow potential shifts in human brain activity.

The model consists of coupled two-variable units as used in mean field modelling in e.g. the Amari model [16] and the Wilson-Cowan model [17]. We added cross-inhibition from each inhibitory population to the excitatory population in the "other" location. With two coupled units the model is:

$$\begin{aligned}
\frac{dEx_1}{dt} &= h_{\text{ex}} - Ex_1 + C_1 \cdot f[Ex_1] - C_2 \cdot f[In_1] + C_{ex} \cdot f[Ex_2] - C_{in} \cdot f[In_2] \\
\frac{dIn_1}{dt} &= h_{\text{in}} - In_1 + C_3 \cdot Ex_1 \\
\frac{dEx_2}{dt} &= h_{\text{ex}} - Ex_2 + C_1 \cdot f[Ex_2] - C_2 \cdot f[In_2] + C_{ex} \cdot f[Ex_1] - C_{in} \cdot f[In_1] \\
\frac{dIn_2}{dt} &= h_{\text{in}} - In_2 + C_3 \cdot Ex_2
\end{aligned} \tag{1}$$

where Ex_i is the activity of an excitatory population, and In_i that of an inhibitory population. The sigmoidal activation function is $f[x] = \frac{1}{1+\varepsilon^{-x}}$ where $x = Ex, In$, respectively, and $\varepsilon = 1000$. Parameters: $h_{ex} = -0.15, h_{in} = -3.95, C_1 = 3.5, C_2 = 2, C_3 = 6.$ C_{ex} and C_{in} are specified in the caption of Fig. 2.

To simulate an arbitrary number *N* of coupled units along one spatial dimension we use the two-variable unit from above in the form:

$$\begin{aligned}
\frac{dEx_i}{dt} &= \tau_{ex}(h_{\text{ex}} - Ex_2 + C_1 \cdot f[Ex_i] \; + C_Ex_j \; + \; C_In_j \; + \; C_{\boldsymbol{noise}} \cdot \zeta_i \\
\frac{dIn_i}{dt} &= \tau_{\text{in}}(h_{\text{in}} - In_i + C_3 \cdot Ex_i)
\end{aligned} \tag{2}$$

with $i = 1, \ldots N$ where *N* is the number of units to be connected. We picked N to be a number of contacts on an sEEG electrode. The coupling matrices for each unit (with N>3) are defined as:

$$C\_Ex_j \; = \; C_{ex} \cdot (f[Ex_{i+1}] \; + \; f[Ex_{i-1}] + \; 0.5f \cdot [Ex_{i+2}] - \; 0.5f \cdot [Ex_{i-2}])$$

$$C\_In_j \; = \; C_{in} \cdot (f[In_{i+1}] \; + \; f[In_{i-1}] + \; 0.5f \cdot [In_{i+2}] - \; 0.5f \cdot [In_{i-2}])$$

i.e. there is cross-coupling with immediate neighbours and cross-coupling at half that strength with next-nearest neighbours. Units further away are not directly coupled. (If the model was used for a space-continuous neural field simulation, a coupling kernel with exponential decay (as e.g. in the Amari model) could be chosen [16]). To avoid boundary-induced spatial asymmetry, boundary conditions are chosen to be periodic, making the model spatially symmetric. Parameters are as for eq. (1), except for the coupling. ζ_i is additive Gaussian noise (mean 0, standard deviation 1), chosen independently for each oscillator *i*. $C_{\boldsymbol{noise}} = 4$.

All simulations were done using Python 3.9 with integration package 'odeint' from the SciPy Library. Noise was generated using a Numpy random number generator. The probability distribution was obtained as in the case of the sEEG data. Illustrations were created with the Python Matplotlib library.

Fig. 1 displays time series and heatmaps of the time series of 20 seconds of a bipolar recording from one sEEG electrode. Slow (< 1Hz) potential shifts as evidenced by the fluctuations in the time series (A) and the heatmap (B) appear in the first four recordings (the deepest contacts) and are consistently lacking in the four other traces. We confirmed that none of these contacts contained other identifiable artifacts outside of seizure activity [18]. The colours in the heatmap show that the slow shifts appear with a polarity reversal from one series to another indicating localised occurrence of the underlying currents. Note, however, that the polarity pattern can switch (red and blue in all four channels reversed at around 38 secs into the segment). Such strong amplitude patterns are not seen in the other four channels. This restriction of slow potential changes with large amplitude remained restricted to the first four contacts over the period of days. Throughout the sEEG (122 bipolar time series in total), anatomical locations of recordings with slow potential shifts showed a considerable degree of consistency over long time scales (hours to days) in that they appeared in the same or similar locations. Shifts of this type were found in a fraction of channels in patients with different epilepsy syndromes (we checked patients with hippocampal sclerosis, focal cortical dysplasia, and tumor-related epilepsy), each of which had tailored implantations, i.e. recordings obtained from different brain structures. In contrast, the appearance of the times series and their frequency content in the usual range of EEG analysis (> 1Hz) was remarkably similar when excluding segments with epileptic seizure rhythms or interictal epileptiform discharges. Comparing the appearance of the slow shifts across different segments and patients we see that while they are spatially stable, their individual patterns of recurrence vary. Fig. 1 can be considered typical but we have also seen rhythmic appearances as well as long isolated shifts. The common feature is that they occur irregularly and are apparently unpredictable. The probability distribution (Fig. 1C) shows a single maximum compatible with a normal distribution for channels without (left) and the appearance of two new maxima in channels with slow shifts (right).

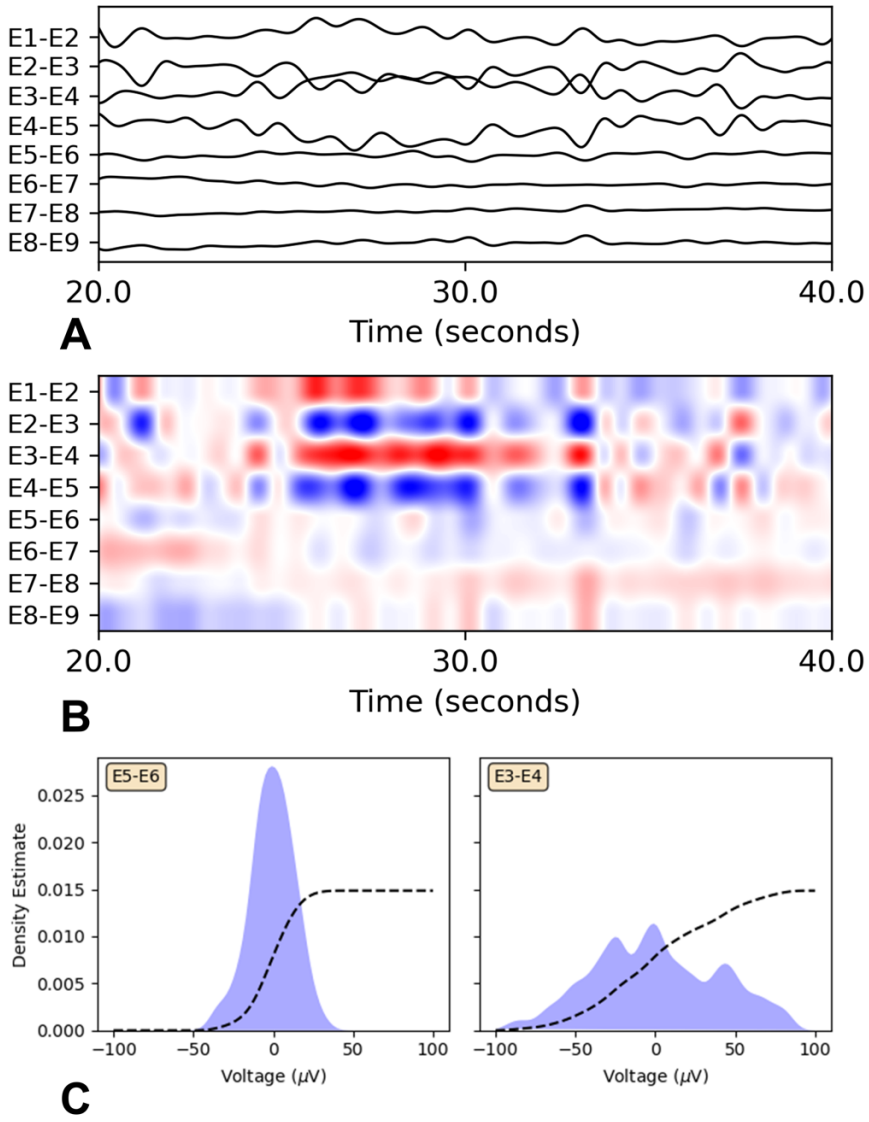

Fig. 1. Time series (A), heatmap (B), and probability distribution (C) of low-pass-filtered (<1Hz) invasive EEG from 8 channels of a single stereo-electrode (called "E", placed in the parahippocampal gyrus) in bipolar montage. The labels indicate the names of the contacts of electrode. The potential shifts, visible in the heatmap B as blue (negative) and red (positive) potential appear most strongly in the first four time series from that electrode.

Following these observations in invasive EEG, we hypothesized that the observed spontaneous slow voltage shifts might be the result of specific localised dynamic interactions instead of being tied to specific abnormal neuroanatomical structures (like a scar). As such the consistently localised and non-propagating slow shifts are compatible with a local spatial symmetry breaking instability. Such instabilities were proposed in the presence of inhibitory coupling in field equations by Turing [19]

but have subsequently been identified as generic features of coupled nonlinear models as a discrete approximation of a field [20]. We thus searched for such instabilities in canonic models of interacting excitatory and inhibitory neural populations [21]. We picked a model of the class that describes macroscopic EEG dynamics and that was used to explain epileptic rhythms as recorded in invasive EEG [12]. A single unit is a nonlinear oscillator with two variables [22]. We prepared the case of two coupled units (representing two nearby locations) with excitatory coupling. We found that in this case both simple and complex oscillations can be simulated but there is no evidence of spatial symmetry breaking instabilities. Following Turing's idea of a competition between activating and inhibitory diffusion [19], we studied the model with both excitatory and inhibitory coupling between units. This is a plausible assumption for locally connected populations with inhibitory interneurons forming synapsis onto excitatory pyramidal neurons. It is not typically included in large scale models of EEG but is a sensible assumption for neighboring contacts with distances on the order of at most a few millimeters).

We studied the impact of symmetric inhibitory cross-coupling for excitatory coupling between populations set to either zero or some finite value. Fig. 2A shows bifurcation diagrams with the behaviour of the two coupled units as a function of the cross-inhibitory coupling constant. In Fig. 2A (top) there is a spatially homogeneous steady state throughout the scanned range of coupling (black dots). As the inhibitory coupling is increased from zero, two additional steady states appear at around 0.038, which results in a tristable state for stronger couplings. Each of the two new states is asymmetric in space. For instance, a positive value in the excitatory population of one two-variable unit is accompanied by a negative value in the other in one case, and *vice versa* in the other, e.g. if unit 1 is in the red state, unit 2 will assume the blue state. The two steady states are strictly antisymmetric to each other, i.e. of Turing-type. The two new steady states appear in simultaneous saddle-node bifurcations with stable nodes and three-dimensional saddles as separatrices. The two newly created attracting nodes both have two real negative eigenvalues and a pair of complex eigenvalues with negative real part. In Fig. 2A (bottom), with additional cross-excitatory coupling, the background state bifurcates to Hopf oscillations but Turing states appear in the same way as in Fig. 2A (top). In the present context, the important feature of this Turing-type bifurcation is that it appears without instability of the original spatially symmetric attractor, i.e. subcritically. The consequence is that there is a parameter region at values of the cross-inhibitory coupling constant before the onset of the asymmetric states where the model is excitable, similar to the case of a standard subcritical saddle-node bifurcation. In this particular excitable state, pulse perturbations can lead to prolonged transients due to the vicinity (in parameter space) of the new stable steady states. And because these steady states are spatially asymmetric, so are their corresponding transients.

Fig 2B shows a scan of local pulse perturbations to the spatially symmetric state without excitatory coupling (c.f. Fig. 2A, top). The excitatory (horizontal) and the inhibitory (vertical) population of unit 1 are perturbed with a short rectangular pulse

and the colour represents a measure of the strength and length of the transient. It is calculated as the temporal integral of differences from the homogeneous steady state. The white and lightly colored regions represent damped oscillatory return to the steady state with an approximately exponentially decaying amplitude. The dark red and dark blue regions represent regions in perturbation space that represent transients of the form of either of the two "ghosts" of the (unstable) spatially asymmetric steady states. The red region is where the excitatory variable of unit 1 transiently stays near the positive (red) branch of diagram 2A (and a negative value of the excitatory variable of unit 2) and the blue region is where the excitatory variable of unit 1 transiently stays near the negative (blue) branch of diagram 2A (and a positive value of the excitatory variable of unit 2). The figure can thus be viewed as a "blurred" version of the actual tristable case (nearby in parameter space) which would show three sharply separated basins of attraction.

Fig 2C is a time series of a simulation of the spatially homogeneous attracting state (left) and the response of that state to a single-pulse perturbation ("Pert") with perturbation parameters chosen in the red region of Fig. 2B. The time series of the two excitatory variables (top 2 graphs) and the heatmap of both (bottom graph) show a prolonged, spatially asymmetric transient which spontaneously decays to the original spatially symmetric steady state. Depending on the polarity of the pulse, an antisymmetric response of similar duration (blue and red colours in the heatmap swapped) can be obtained for perturbation parameters set in the blue region of Fig 2B. The damped oscillatory response after the spatially asymmetric transient is due to the vicinity of a supercritical Hopf bifurcation as previously used to model a small amplitude seizure onset [12]. We propose to call these prolonged non-oscillatory transients Turing-type transients (TTT), We have extensively studied the model eq. (1) with two coupled E-I units and confirmed that the cross-inhibitory coupling-induced transients arise generically in the vicinity of an oscillatory onset and that the spatially homogeneous "background" state may either be a steady state or oscillatory. As such, spatially asymmetric transients of the type shown in Fig. 2C and 2D do not dependent on specific background dynamics.

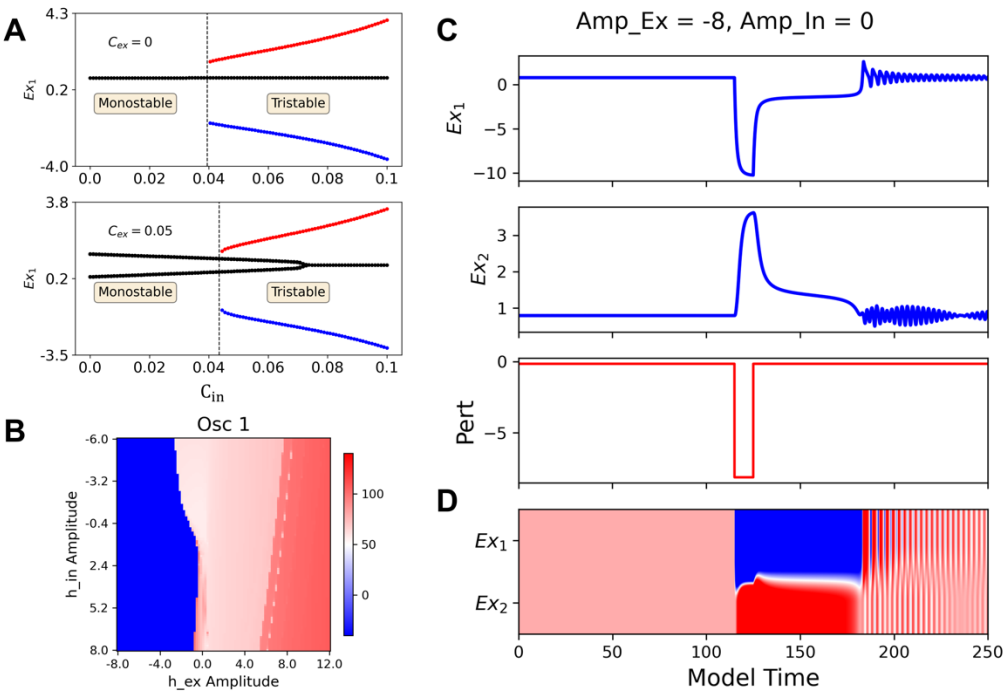

Fig. 2. Modelling of the occurrence of spatial symmetry breaking instabilities in dynamical system eq. (1) composed of two symmetrically coupled oscillators with cross excitation and cross-inhibition. A) Bifurcation diagram of eq. (1) with tristability as a function of inhibitory coupling C_{in} for C_{ex}= 0 (top) and C_{ex}= 0.05 (bottom). The figure is composed of simulations starting from two different initial conditions. The red branch plus the black branch is the solution for initial conditions where oscillator one starts in the 'upper' state, and oscillator two in the 'lower' state. The blue branch plus the black branch is the solution for initial conditions where oscillator one is in the 'lower' state, oscillator two in the 'upper' state (both starting at C_{in}= 0.1). The black line is the spatially homogenous state throughout for C_{ex}= 0 (top) and the homogeneous steady state branching to a Hopf oscillation for C_{ex}= 0.05 (bottom). B) Scan of perturbation parameters for eq. (1) when oscillator 1 is perturbed in the excitatory (horizontal) and the inhibitory (vertical) input. The model is prepared in the monostable state at C_{in}= 0.036 near the onset of the tristability. Colour-coded is the integral of the transient deviation from the homogenous steady state. Blue and red are negative and positive relative to steady state, respectively. C) Response of model eq. (1) in the excitable monostable state in B) to a pulse perturbation at C_{ex}= 0. Shown are the time series of the excitatory variables of both oscillators (top and centre), and the pulse protocol (bottom). The damped oscillatory response after the cessation of the transient spatially asymmetric state is due to the vicinity of a Hopf bifurcation (cf. Fig. 2A). D) Heatmap of both excitatory variables with pulse perturbation as in C. Pulse width: 10 model time units; pulse amplitude: h_{ex_1}= -8, h_{in_1}= 0 (applied to oscillator 1 only), c.f. Fig. 2B).

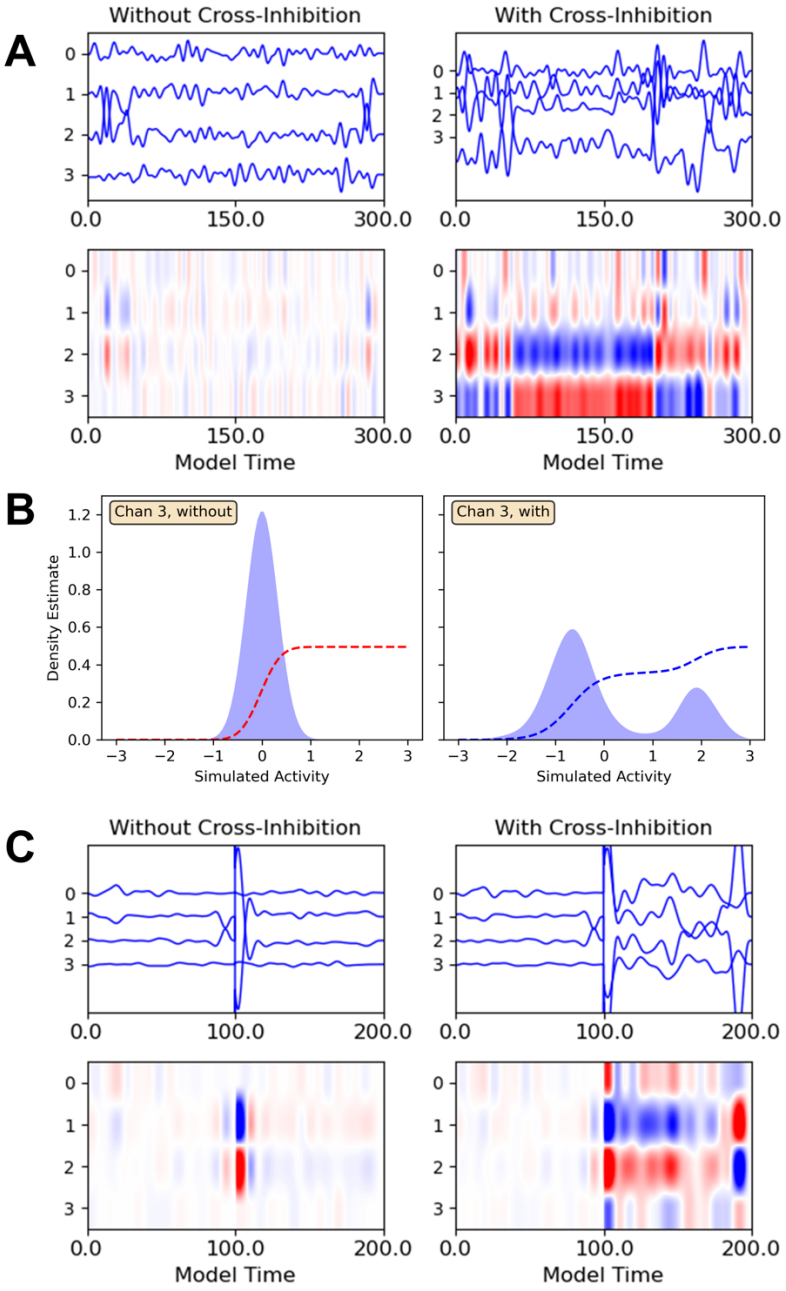

Fig. 3. Modelling of the model of five coupled units according to eq. 2, with cross-excitatory coupling and in the presence of noise. Simulations are done in the absence and in the presence of cross-inhibitory coupling. Shown is the simulated bipolar montage of the low-pass filtered excitatory variables, comparable to the sEEG in Fig. 1. A) Time series and heatmaps of fluctuations in the monostable state in the absence (left) and presence (right) of cross-inhibitory coupling. B) Kernel density estimate (blue) and cumulative function (red) of the time series in A). Left: without; Right: with cross-inhibitory coupling. C) Simulation of the model eq. (2) as in A) but with pulse perturbation added at 100 model time units. Coupling: C_{ex}= 0.1. C_{in}= 0 (without) and C_{in}= 0.16 (with). Other parameters as specified in the text.

Fig. 3A (left) shows time series of the excitatory variables in bipolar montage for eq. (2) with N=5 (to simulate four times series in bipolar montage as in Fig. 1). In the absence of cross-inhibitory coupling the dynamics is noise dominated in all channels. No strong oscillatory contribution from the stable focus of the model is seen due to low-pass filtering in either the time series 3A (left top), or the heatmap 3A (left bottom), c.f. Fig. 1, bottom four channels. Fig. 3A (right) shows corresponding time series when cross-inhibitory coupling is added. Under otherwise identical conditions, the presence of cross-inhibitory coupling leads to slow amplitude fluctuations in the time series (3A, right top) and the strong colours in the corresponding heatmap (3A, right bottom). The presence of Turing-type transients in Fig. 3 is due to the vicinity of the subcritical Turing instability. This adds irregular large voltage fluctuations to the signal and occasionally results in switching of polarity.

The analysis of the time series without cross-inhibitory coupling (Fig. 3B, left) shows a normally distributed histogram around zero voltages, and the corresponding sigmoidal cumulative distribution with a single inflection point. In contrast, the analysis of the time series with cross-inhibitory coupling (Fig. 3B, right) shows a two-peak distribution with both maxima away from zero voltages and a cumulative distribution with two inflection points. The low-pass filter setting was able to remove the near-zero components of the central steady state entirely. The simulation of the model with a rectangular pulse in Fig. 3C shows short-lived transients immediately following the pulse with no cross-inhibition (left) and a long-lived spatially asymmetric transient with noisy fluctuations superimposed with added cross-inhibition (right). Note the spontaneous phase reversal due to noise towards the end of the simulation, at around 190 model time units. The slow shifts remain localised and do not propagate to adjacent locations.

Slow potential shifts (below 1Hz) are seen in human cortical and subcortical structures in invasive EEG with remarkable spatial stability but always displaying temporal irregularity (Fig. 1). This presents a puzzle to previous theories approaches which focussed on solutions which typically propagate in space and which also show regularity in their temporal appearance (in the absence of noise terms) [23]. We simplified the mathematical modelling problem to describe a spatial neural field to the case of two coupled nonlinear units with excitatory and inhibitory cross-coupling (Eq. 1). This is analogous to the study of spatial symmetry breaking instabilities of Turing-type reaction-diffusion equations (PDEs) by means of two coupled biochemical oscillators [20]. We find a symmetry-breaking instability of a homogeneous steady state which occurs subcritically [24], i.e. generating a parameter region with tristability of the homogenous state with two antisymmetric spatially asymmetric states (Fig. 2A). This leads to the associated feature of Turing-type excitability (in nearby parameter space) with spatial symmetry breaking transients (Fig. 3A and C). Excitability allows for two ways of inducing these localised and self-terminating potential shifts. Pulse stimulation to the state space region associated with either of the spatially asymmetry states; or added noisy fluctuations, strong enough to occasionally achieve supra-threshold responses (Fig

2C). If we model the EEG background state as a noisy spatially homogenous state, then the Turing-type instability imposed by cross-inhibitory coupling allows for Turing-type excitability and thus irregular slow shifts of the simulated EEG (Fig. 3A). The model makes explicit predictions about e.g. the histograms (Fig. 3B) of the slow components.

We modelled the case of four iEEG signals from a single electrode with a model of five locations and corresponding bipolar montage (Fig. 3). We find the Turing-type excitability after appropriate rescaling of coupling parameters. With adjustment of the inhibitory cross-coupling strength, we are able to create dynamics without and with localised irregular slow shifts similar to those seen in the EEG (Fig. 3A). While we can make no claim here about whether the mechanism actually underlies slow shifts in the EEG, we offer a novel hypothesis of the dynamical origin of spatially consistent slow voltage shifts in different anatomical regions in the human brain. The appearance of slow shifts in cortical and subcortical regions that are far apart (distances in the order of centimetres between the stereo electrodes) is potentially consistent with a long-range neural field approach as recently postulated from the analysis of a large number of experimental fMRI images [25].

Unlike in animal models, it is not possible to do explicit hypothesis testing of individual model components in the context of clinical presurgical monitoring. It is, however, possible to computationally predict responses of electrical pulse stimulation as used clinically to e.g. identify eloquent cortex [26]. Three particular predictions for iEEG analysis follow from our model: i) iEEG channels with slow potential shifts should show broad histograms with multiple inflection points in the cumulative curve if appropriately low-pass filtered; ii) an appropriate single-pulse perturbation of a slow-shift contact should lead to a prolonged voltage transient in a reproducible direction (see e.g. Figs. 2C and 3C); iii) if the EEG is in a state of large amplitude at the moment of stimulation, a single-pulse perturbation of a slow-shift contact could lead to the reverse (transient) potential shift. Also, there should not be propagation of slow shifts to adjacent contacts as expected e.g. for excitable systems without Turing instability. The reason is that the antisymmetric Turing instability actively prohibits propagation to other units by cross-inhibition (similar to the case of stationary patterns in space-continuous neural field models [27]).

We can speculate on possible functional roles of slow potential shifts during ongoing brain activity. The localisation and duration of those shifts could suggest that a state of tristability with distinct spatial asymmetries that can be maintained for a certain amount of time, and thus used as an information processing unit. Being excitable, Turing-type transients show threshold features like, for instance, neurons. However, in addition to the all-or-none response in neurons, Turing-type transients are of the either-or-ignore type: depending on the perturbing stimulus they can either not respond (0) or respond in one (+1) or another (-1) way. The temporal transient that maintains a spatial voltage gradient for some amount of time (here on the order of seconds), e.g. following sensory stimulation [10], presents a novel means of input-dependent decision making

in one direction or another. The spatial gradients in the time series of Fig. 1B might then allow for differential downstream processing based on the polarity of the underlying gradient and associated ionic currents.

ACKNOWLEDGMENTS

This research was supported by the National Natural Science Foundation of China (grants 12072021, 12102014, 11932003) and the Fundamental Research Funds for the Central Universities and the Youth Teacher International Exchange & Growth Program (No. QNXM20220049).

References

1. Wu, S., et al., *Direct Current Shift Recordings*, in *Invasive Studies of the Human Epileptic Brain: Principles and Practice*, S.D. Lhatoo, Editor. 2018, Oxford University Press.
2. Wu, S., et al., *Role of ictal baseline shifts and ictal high-frequency oscillations in stereo-electroencephalography analysis of mesial temporal lobe seizures.* Epilepsia, 2014. **55**(5): p. 690-698.
3. Khoo, H.M., et al., *Technical Aspects of SEEG and Its Interpretation in the Delineation of the Epileptogenic Zone.* Neurol Med Chir (Tokyo), 2020. **60**(12): p. 565-580.
4. Bowyer, S.M., et al., *Slow brain activity (ISA/DC) detected by MEG.* J Clin Neurophysiol, 2012. **29**(4): p. 320-6.
5. Chernysheva, V.A., *[Dynamics of slow potential changes in human subcortical structures during mental activity under conditions of directed changes in the brain internal medium].* Fiziol Zh SSSR Im I M Sechenova, 1971. **57**(2): p. 150-8.
6. McCallum, W.C., et al., *Event related slow potential changes in human brain stem.* Nature, 1973. **242**(5398): p. 465-7.
7. Lee, S., et al., *DC shifts, high frequency oscillations, ripples and fast ripples in relation to the seizure onset zone.* Seizure, 2020. **77**: p. 52-58.
8. Kanazawa, K., et al., *Intracranially recorded ictal direct current shifts may precede high frequency oscillations in human epilepsy.* Clin Neurophysiol, 2015. **126**(1): p. 47-59.
9. Kotchoubey, B., et al., *Modification of slow cortical potentials in patients with refractory epilepsy: a controlled outcome study.* Epilepsia, 2001. **42**(3): p. 406-16.
10. Lang, W., et al., *Cortical DC potential shifts accompanying auditory and visual short-term memory.* Electroencephalogr Clin Neurophysiol, 1992. **82**(4): p. 285-95.
11. Jirsa, V.K., et al., *On the nature of seizure dynamics.* Brain, 2014. **137**(Pt 8): p. 2210-30.
12. Zhang, L., Q. Wang, and G. Baier, *Spontaneous transitions to focal-onset epileptic seizures: A dynamical study.* Chaos, 2020. **30**(10): p. 103114.
13. Proix, T., et al., *Predicting the spatiotemporal diversity of seizure propagation and termination in human focal epilepsy.* Nat Commun, 2018. **9**(1): p. 1088.
14. Liou, J.Y., et al., *A model for focal seizure onset, propagation, evolution, and progression.* Elife, 2020. **9**.
15. Steyn-Ross, M.L., Steyn-Ross, D. A., Sleigh, J.W. , *Interacting Turing-Hopf Instabilities Drive Symmetry-Breaking Transitions in a Mean-Field Model of the Cortex: A Mechanism for the Slow Oscillation.* Physical Review X, 2013. **3**: p. 021005.
16. Taylor, P.N. and G. Baier, *A spatially extended model for macroscopic spike-wave discharges.* J Comput Neurosci, 2011. **31**(3): p. 679-84.

17. Wang, Y., et al., *Phase space approach for modeling of epileptic dynamics.* Phys Rev E Stat Nonlin Soft Matter Phys, 2012. **85**(6 Pt 1): p. 061918.
18. Diehl, B. and C.A. Scott, *Physiological Activity and Artefacts in Epileptic Brain in Subdural EEG*, in *Invasive Studies of the Human Epileptic Brain: Principles and Practice*, S.D.L.e.e. al., Editor. 2018, Oxford University Press.
19. Turing, A.M., *The chemical basis of morphogenesis.* Bull Math Biol, 1953. **52**(1-2): p. 153-97; discussion 119-52.
20. Roessler, O.E., Seelig, F.F., *A Rashevsky-Turing System as a Two-cellular Flip-flop.* Zeitschrift für Naturforschung, 1972. **27b**: p. 1444.
21. Deco, G., et al., *The dynamic brain: from spiking neurons to neural masses and cortical fields.* PLoS Comput Biol, 2008. **4**(8): p. e1000092.
22. Izhikevich, E.M., *Dynamical systems in neuroscience : the geometry of excitability and bursting*. Computational neuroscience. 2007, Cambridge, Mass.: MIT Press. xvi, 441 p.
23. Goodfellow, M., K. Schindler, and G. Baier, *Self-organised transients in a neural mass model of epileptogenic tissue dynamics.* Neuroimage, 2012. **59**: p. 2644-2660.
24. Vanag, V.K. and I.R. Epstein, *Subcritical wave instability in reaction-diffusion systems.* J Chem Phys, 2004. **121**(2): p. 890-4.
25. Pang, J.C., et al., *Geometric constraints on human brain function.* Nature, 2023. **618**(7965): p. 566-574.
26. Kovac, S., P. Kahane, and B. Diehl, *Seizures induced by direct electrical cortical stimulation--Mechanisms and clinical considerations.* Clin Neurophysiol, 2016. **127**(1): p. 31-39.
27. Wilson, H.R. and J.D. Cowan, *A mathematical theory of the functional dynamics of cortical and thalamic nervous tissue.* Kybernetik, 1973. **13**(2): p. 55-80.